

Randomness, Maxwellian Distributions, and Resonance Absorption

B. Bezzerides, S. J. Gitomer, and D. W. Forslund

Los Alamos Scientific Laboratory, University of California, Los Alamos, New Mexico 87545

(Received 16 November 1979)

A capacitor-model plasma simulation and test-particle methods have been utilized to study energy distributions of electrons heated by resonance absorption of intense laser light. Certain subtle properties of the resonantly excited field which introduce a random character to the heating and have a controlling influence on the shape of the distribution have been identified.

The generation of hot electrons in high-intensity laser experiments has received attention in the last few years.¹ Particle simulations have concentrated on resonant absorption as the dominant absorption mechanism.² One important conclusion of the simulations is that for a wide range of conditions, the time-averaged electron distribution function is well approximated by a two-temperature Maxwellian consisting of the background thermal distribution and a low-density high-energy Maxwellian with a "temperature" T_{hot} . Although considerable progress has been made in obtaining scaling laws for T_{hot} from the simulations, the microscopic processes responsible for the heating and the composition of the time-averaged distribution have received only cursory attention. Previous work on modeling the hot-electron production relied on the assumption of temporally periodic standing-wave fields.³ In fact, the fully self-consistent fields of the simulation are aperiodic and traveling, showing a rich frequency content when spectrally analyzed. In Ref. 3, the detailed shape of the heated distribution is a direct result of the use of a cold Maxwellian source. Our work shows that it is the aperiodic behavior of the fields themselves which leads to the final hot-electron distribution.

In this Letter our electric fields are drawn from one-dimensional (1D) capacitor-model simulations of resonant absorption with a uniform driver E_0 and a fixed linear ramp density profile of scale length L . In Fig. 1 a typical run is displayed showing the power spectrum at various spatial points. Two distinctive features of Fig. 1 should be noted. First, one observes the presence of multiple harmonics of the pump frequency ω_0 , a manifestation of nonlinear steepening. In the corresponding 2D problem, these harmonics would provide a source for higher-harmonic radiation.⁴ Second, we see the aperiodic response of the plasma at the local plasma frequency, i.e., for $\omega_{pe}/\omega_0 < 1$ (> 1) modes appear with frequency less than (greater than) the driver frequency. As

is well known, oscillations at the free modes of a damped linear driven oscillator dissipate in time leaving only a response at the driving frequency. We find, however, that the enhanced free-mode response shown in Fig. 1 is a persistent feature of all our self-consistent simulations.

To determine what role the aperiodic field plays in generating the observed hot-electron distribution, we utilize some novel test-particle schemes and associated diagnostics. Test particles are loaded into the computational region exactly as in a self-consistent simulation. The particles move, however, *independently* of one another in a *prescribed* electrostatic field. As a consistency check, we ran such a test-particle calculation using the field from an entire self-consistent simulation and obtained exactly the same time-averaged hot-electron spectrum as in the original simulation. On the other hand, using the field

$$P(E(x, t)) = \sum_{n=0}^N E(x, t - 2\pi n/\omega_0) / (N + 1)$$

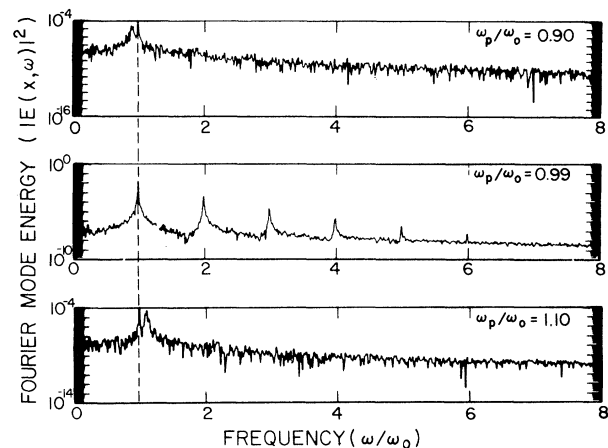


FIG. 1. Fourier power spectrum $|E(x, \omega/\omega_0)|^2$ vs ω/ω_0 for positions corresponding to $\omega_{pe}/\omega_0 = 0.90$, 0.99 and 1.10. Simulation parameters used were background temperature 640 eV, $0 \leq x\omega_0/c \leq 20$, $k_0 L = 12.5$, 179 spatial cells, $E_0 = 0.002$, and 32 timesteps per driver period.

projecting out the periodic component, we obtain a hot-electron distribution function which exhibits order-of-magnitude deviations from a Maxwellian. Comparing this result with that of the full simulation field in Fig. 2, we conclude that $\delta E = (1-P)E$, the aperiodic part of the field, although small compared to the peak amplitude of the field, plays a critical role in establishing the shape of the hot-electron distribution. It is a general result that without the aperiodic content to the field *the detailed Maxwellian feature is lost* and it is no longer appropriate to define a T_{hot} .

Local monitoring of the heating in phase space permits an even more detailed comparative analysis of the role of the aperiodic fields. Snapshots of phase space show the quasiperiodic nature of the heating. During each cycle of the driving field, a burst of hot-electrons streams out of the large-amplitude field region and is collected at the problem boundary to form the time-averaged distribution which is a result of many such cycles. In Fig. 3(a), we record the velocity versus time for all particles with $(v/c)^2 \geq 0.09$ as they stream in and out of a fixed spatial region localized about the large-amplitude field. The example chosen is for a self-consistent simulation. As expected, the acceleration of particles *within a given cycle* is consistent with the model of resonant acceleration in a coherent field. However, the most striking feature of Fig. 3(a) is the almost random spectrum of velocities present from cycle to cycle.

In Fig. 3(b) we plot the average energy per particle within the monitored region as a function of time. The displays of Fig. 3 illustrate the almost random character of the heating process even for this energy moment. For the case of

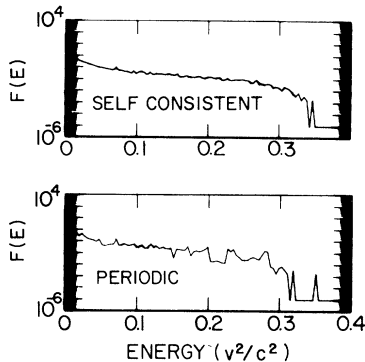


FIG. 2. Time-averaged distribution functions $f(E)$ vs E for (a) a self-consistent simulation and (b) a periodic test-particle calculation.

periodic applied fields (a test-particle calculation), a similar analysis was performed. The anticipated result, namely, that each cycle is completely equivalent, is obscured because of too few simulation particles. To determine just how the results for the periodic and aperiodic cases differ, we performed a statistical analysis of the average-energy maxima for the two cases in which the number N of simulation particles was varied. In Fig. 4(a), we plot a histogram of average-energy maxima for a self-consistent simulation. The standard deviation σ for a number of such aperiodic and periodic runs is plotted in Fig. 4(b) vs N . The periodic runs show a $1/N^{1/2}$ statistical dependence, a signature of numerical rather than physical effects.⁵ However, the self-consistent simulations (aperiodic) show σ independent of N for $N \geq 40\,000$, suggesting that the randomness of the maximum average energy per heated particle is of a dynamical origin. It is worthwhile to note that the mean average energy per particle ϵ agrees with that obtained by assuming a Maxwellian tail, $\epsilon = T_{\text{hot}} [1 + 2b \exp(-b^2) / \pi^{1/2} \text{erfc}(b)]$, where $b = (v_{\text{min}}/c) / (2T_{\text{hot}})^{1/2}$ and T_{hot} in units of mc^2 is the measured temperature of a self-consistent simulation.

Additional evidence of the intrinsic randomness is obtained by a different test-particle scheme in which particles are injected into the computational box by means of a spatially uniform beam with a definite beam velocity. This method of injection

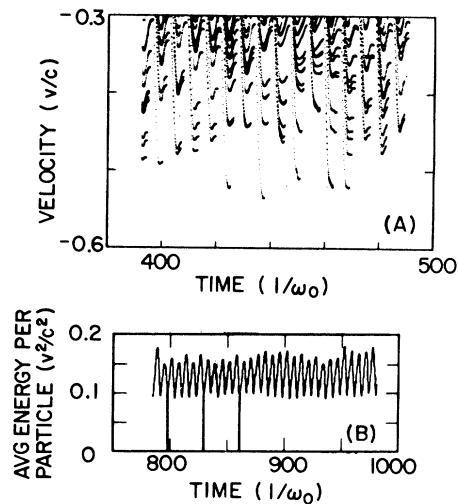


FIG. 3. (a) Velocity vs time for particles in phase-space region with position $14.25 \leq x\omega_0/c \leq 16.75$ and velocity $-0.6 \leq v/c \leq -0.3$. (b) Average energy per particle in phase-space region above vs time.

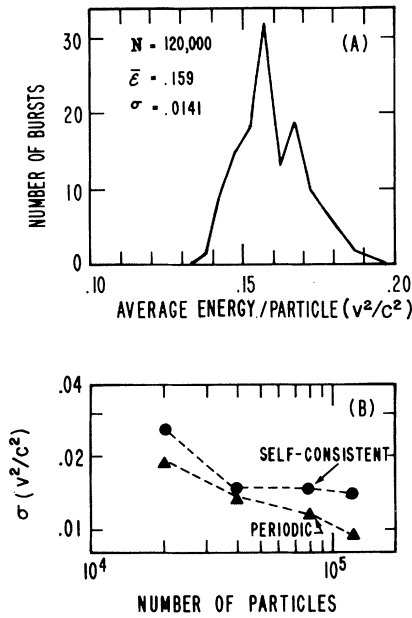


FIG. 4. (a) Pulse-height analysis of Fig. 3(b) data. Number of pulses vs pulse height. (b) Standard deviation of data from (a) vs number of simulation particles for self-consistent simulations and periodic test-particle calculations.

tion should be compared with the previous test-particle approach in which particles are injected randomly from the thermal distribution. The steady injection removes one source of randomness and allows a systematic probing of the heating characteristics of the field. Particles are collected, after passing through the heating region, at a spatial point near enough to the heating region to avoid collection of hot particles originating from a later heating cycle. Thus we can construct a distribution of hot particles for a given beam velocity created during a given heating cycle. This allows us to analyze the cycle-by-cycle composition of the time-averaged distribution function.

In Fig. 5 we show (a) the distribution of hot particles for three different cycles and (b) the time-averaged distribution for over 30 cycles of the simulation electric field with a beam velocity set at $v_{beam}/c = 0.08$. The figure shows clearly that the time-averaged distribution (in this case a Maxwellian with a tail temperature equal to the simulation T_{hot}) comes about by the averaging of all the single-particle distributions which themselves fluctuate in an almost random fashion. The results for other beam velocities show the same general features. The time-averaged dis-

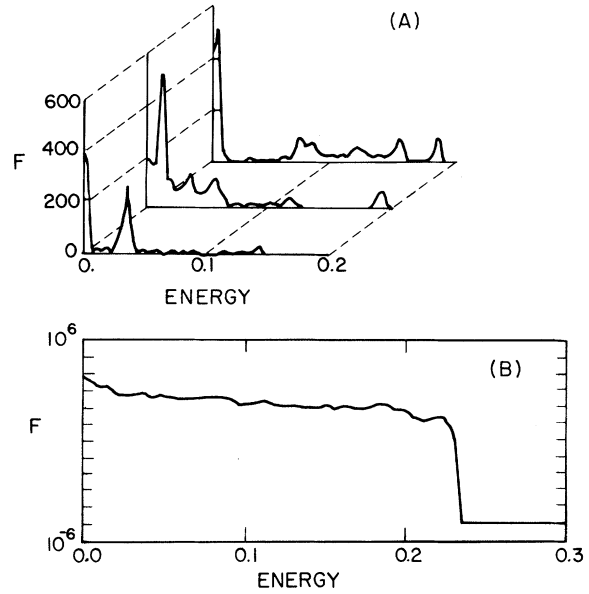


FIG. 5. Hot-electron distributions due to an injected beam with velocity $v/c = -0.08$. (a) Distributions for three different heating cycles and (b) time-averaged distribution due to over 30 heating cycles.

tribution of the simulation, of course, is obtained by averaging the result of all the beams, each weighted by the initial Maxwellian. From this result it is tempting to speculate that the Maxwellian character of the hot-electron distribution observed in self-consistent simulations of resonant absorption is directly related to the random fluctuations in the distribution of hot particles produced from cycle to cycle. Certainly, without this element of randomness, it would be very difficult to understand this observation.

The random fluctuations in the hot-electron distribution function from cycle to cycle have been shown to be due to aperiodic- or free-mode frequency components of the field. To see how these excitations are self-consistently related to the production of hot electrons, we turn to the fully nonlinear equation for the electrostatic field coupled to the capacitor field. The coupling to the particles enters through the pressure $P(x, t)$ which is in turn coupled to the heat flux $Q(x, t)$ through

$$\left(\frac{\partial}{\partial t} + v \frac{\partial}{\partial x}\right) \frac{P}{n^3} = -\frac{1}{n^3} \frac{\partial Q}{\partial x}, \quad (1)$$

where $v(x, t)$ and $n(x, t)$ are the local fluid velocity

and density, and

$$Q(x,t) = m \int dv [v - v(x,t)]^2 f(x,v,t).$$

The field equation was solved numerically where P was obtained from (1) with $\partial Q/\partial x = 0$, i.e., in the adiabatic limit. As in the case of the simulations, the solutions showed excitations at the driving frequency and several higher harmonics. However, except for some initial transients, *there was no free-mode response*, the nonlinear convection having damped these modes out. The same result is obtained using a linearized form of Q (Landau damping). Thus we see that it is the contribution to Q due to the pulselike production of hot electrons which leads to a pressure P that ultimately acts as an additional source for the electrostatic field—an aperiodic source.

The authors gratefully acknowledge the contributions of D. F. DuBois to an early stage of this work. Helpful discussions with A. Petschek were

greatly appreciated. This work was performed under the auspices of the U. S. Department of Energy.

¹K. R. Manes *et al.*, Phys. Rev. Lett. **39**, 281 (1977); R. P. Godwin, P. Sachsenmaier, and R. Sigel, Phys. Rev. Lett. **39**, 1198 (1977).

²D. W. Forslund, J. M. Kindel, and K. Lee, Phys. Rev. Lett. **39**, 284 (1977); K. Estabrook and W. L. Kruer, Phys. Rev. Lett. **40**, 42 (1978).

³P. DeNeef and J. S. DeGroot, Phys. Fluids **20**, 1074 (1977).

⁴N. H. Burnett *et al.*, Appl. Phys. Lett. **31**, 172 (1977); E. A. McLean *et al.*, Appl. Phys. Lett. **31**, 825 (1978).

⁵C. K. Birdsall, A. B. Langdon, and H. Okuda, in *Methods in Computational Physics*, edited by B. Alder, S. Fernbach, and M. Rotenberg (Academic, New York, 1970), Vol. 9, p. 241.

Long-Time Containment of a Pure Electron Plasma

J. H. Malmberg and C. F. Driscoll

Department of Physics, University of California, San Diego, La Jolla, California 92093

(Received 15 January 1980)

A pure electron plasma has been confined in cylindrical geometry for many minutes. Confinement scalings with background pressure and magnetic field show that the maximum confinement times, while long, are 100–5000 times shorter than the limit set by electron-neutral collisions.

A single-species plasma is fundamentally different from a two-component plasma in that a single species can, in theory, be confined indefinitely. Here, we consider a cylindrical confinement geometry with an axial magnetic field. Like-particle interactions, however complex and nonlinear, cannot cause the plasma to expand radially, because the total canonical angular momentum must be conserved. Rather, it has been shown theoretically that like-particle interactions cause transport to a confined thermal equilibrium state.¹⁻⁴ Radial expansion of the plasma can occur only if external torques act to change the total canonical angular momentum. Such torques may arise from collisions with neutral atoms, angular asymmetries in the magnetic field or containment vessel, finite wall resistance, or radiation effects.

Here, we report experimental results on long-time containment of a pure electron plasma. One-half of the injected electrons are contained for

times $\tau_{1/2} \leq 350$ sec in modest magnetic fields $B \leq 676$ G, with background pressures $P \geq 10^{-10}$ Torr. The scaling of confinement time has been obtained over 7 decades in helium background pressure and $2\frac{1}{2}$ decades in B^2 . At high pressures, the containment scales as expected from transport due to electron-neutral collisions, with significant effects from Joule heating and neutral recoil cooling. At low pressures, the collisional transport time scaling is broken: The observed containment is several decades shorter than expected from binary elastic collisions alone.

The experimental configuration is shown in Fig. 1; the theory of operation has been discussed in detail elsewhere.⁵ Electrons are thermally emitted from a spiral-wound thoriated tungsten filament, which has a radially dependent potential

$$\varphi_f(r) \approx V_b + V_f r^2 / R_f^2. \quad (1)$$

For the present experiment, $V_b = -50$ V, $V_f = 12.4$ V, and the filament has radius $R_f = 1.4$ cm.